JOURNAL OF VIROLOGY, May 1997, p. 3507–3514 Vol. 71, No. 5
0022-538X/97/$04.00+0

Structure-Based Mutagenesis of the Catalytic Domain of Human Immunodeficiency Virus Type 1 Integrase

ALAN ENGELMAN,[1]* YING LIU,[1] HONGMIN CHEN,[1] MICHAEL FARZAN,[1] AND FRED DYDA[2]

Division of Human Retrovirology, Dana-Farber Cancer Institute and Department of Pathology, Harvard Medical School, Boston, Massachusetts 02115,[1] and Laboratory of Molecular Biology, National Institute of Diabetes and Digestive and Kidney Diseases, Bethesda, Maryland 20892[2]

Received 27 November 1996/Accepted 14 January 1997

Two different crystal structures of the human immunodeficiency virus type 1 (HIV-1) integrase (IN) catalytic domain were analyzed for interactions at the enzyme active site. Gln-62 and Glu-92 interact with active-site residue Asp-64, and Lys-136 interacts with active-site residue Asp-116 across a dimer interface. Conservative and nonconservative substitutions were introduced at these positions to probe the roles of these interactions in HIV-1 integration. Purified mutant proteins were assayed for in vitro 3′ processing, DNA strand transfer, and disintegration activities, and HIV-1 mutants were assayed for virion protein composition, reverse transcription, and infectivities in human cell lines. Each of the mutant IN proteins displayed wild-type disintegration activity, indicating that none of the interactions is essential for catalysis. Mutants carrying Gln or Ala for Glu-92 displayed wild-type activities, but substituting Lys for Glu-92 reduced in vitro 3′ processing and DNA strand transfer activities 5- to 10-fold and yielded a replication-defective IN active-site mutant viral phenotype. Substituting Glu for Gln-62 reduced in vitro 3′ processing and DNA strand transfer activities 5- to 10-fold without grossly affecting viral replication kinetics, suggesting that HIV-1 can replicate in T-cell lines with less than the wild-type level of IN activity. The relationship between IN solubility and HIV-1 replication was also investigated. We previously showed that substituting Lys for Phe-185 dramatically increased the solubility of recombinant IN but caused an HIV-1 particle assembly defect. Mutants carrying His at this position displayed increased solubility and wild-type replication kinetics, showing that increased IN solubility per se is not detrimental to virus growth.

Like all retroviruses, human immunodeficiency virus type 1 (HIV-1) integrates a double-stranded DNA copy of viral RNA into host chromosomal DNA. Integration requires two biochemical activities of the virion-associated integrase (IN) protein. The first activity is 3′ processing, wherein IN cuts blunt-ended viral DNA near each 3′ end, adjacent to CA dinucleotides which are conserved in all retroviruses and retrotransposons. IN subsequently joins each recessed 3′ end to the 5′-PO_4 of a double-stranded staggered cut in chromosomal DNA. This second activity is referred to as DNA strand transfer. Repair of the integration intermediate, which requires filling in the single-strand gaps between the unjoined viral 5′ ends and the cut host 3′ ends, as well as joining these ends, yields the integrated provirus flanked by the sequence duplication of the double-stranded cut. At present it is unclear whether viral reverse transcriptase (RT) and IN, and/or host cell enzymes, accomplish these final steps (for a recent review of retroviral integration, see reference 25).

HIV-1 IN purified from a variety of sources displays 3′ processing and DNA strand transfer activities in vitro. Reactions require IN, substrates which mimic the ends of HIV DNA, and either Mg^{2+} or Mn^{2+} (7, 19, 39). IN also displays a third in vitro activity, termed disintegration, which is an apparent reversal of the DNA strand transfer reaction (9). Whereas full-length HIV-1 IN is required for efficient in vitro 3′ processing and DNA strand transfer activities (11, 38, 47), the isolated catalytic domain, encompassing approximately residues 50 to 212 of the 288-residue protein, can catalyze disintegration (6). The catalytic domain contains three amino acid residues, Asp-64, Asp-116, and Glu-152, which comprise the enzyme active site (6, 13, 15, 27, 30, 44, 47).

The three-dimensional structures of the catalytic domains of HIV-1 (13) and avian sarcoma virus (4) INs have been solved by X-ray crystallography. IN belongs to a structurally related superfamily of polynucleotidyltransferases (reviewed in reference 32). All members of this family, which include RNase H, RuvC, and bacterial transposases, catalyze one-step transesterification reactions using Asp and Glu active-site residues. The proposed role of these residues is to bind and coordinate the catalytically essential divalent metal ions.

In this study, we identified three amino acid residues, Gln-62, Glu-92, and Lys-136, which interact with either active-site residue Asp-64 or active-site residue Asp-116 in two different crystal structures of the HIV-1 IN catalytic domain. The roles of these interactions in IN function were probed by studying a series of site-directed mutants. The results indicate that the interactions are not essential for catalysis, suggesting they may play a more significant role in crystal packing than in integration. We also determined that HIV-1 can replicate in T-cell lines with less than the wild-type (WT) level of IN activity and that increased IN solubility does not necessarily inhibit HIV-1 assembly and replication.

MATERIALS AND METHODS

Site-directed mutagenesis. Site-directed mutations were introduced into the IN coding regions of plasmid DNAs by using overlapping PCR as previously described (16, 23). For expression of recombinant IN in *Escherichia coli*, pINSD (15), which encodes IN from the NL4-3 strain of HIV-1, was used as the template. For expression of HIV-1_{NL4-3} in human cell lines, pNL4-3 (1) was used as the template. The presence of mutations was confirmed by dideoxy sequencing (37).

* Corresponding author. Mailing address: Division of Human Retrovirology, Dana-Farber Cancer Institute, 44 Binney St., Boston, MA 02115. Phone: (617) 632 4361. Fax: (617) 632 3113.

Protein expression and purification. Bacterial expression constructs were transformed into *E. coli* BL21(DE3) (41). Cells were grown at 37°C in Terrific broth (1.5 liters) containing 100 μg of ampicillin per ml, and IN expression was induced as previously described (10). Cells were harvested, resuspended in 35 ml of cold 25 mM HEPES (pH 7.6)–0.1 mM EDTA, frozen in liquid N_2, and thawed on ice overnight. The remainder of the preparation was done at 4°C. Cells were harvested, resuspended in 35 ml of buffer A (20 mM Tris-HCl [pH 8.0], 0.5 M NaCl, 2 mM β-mercaptoethanol [β-ME], 0.1 mM EDTA, 5 mM imidazole, 0.2 mg of lysozyme per ml), incubated for 30 min, and then sonicated as previously described (10). The lysate was centrifuged at 40,000 × *g* for 35 min, and the supernatant (fraction I) was saved. The pellet was resuspended by homogenization in 20 ml of buffer B (20 mM Tris-HCl [pH 8.0], 0.5 M NaCl, 6 M guanidine-HCl [Gnd-HCl], 2 mM β-ME, 0.1 mM EDTA, 5 mM imidazole). The suspension was stirred for 30 min and centrifuged at 40,000 × *g* for 35 min, and the supernatant (fraction II) was saved. IN-containing fractions were identified following sodium dodecyl sulfate-polyacrylamide gel electrophoresis (SDS-PAGE) and staining with Coomassie blue.

IN mutants were expressed as fusion proteins containing a 21-residue N-terminal affinity tag with six adjacent histidine residues. The His tag facilitates purification by metal-chelating chromatography (43). The His tag was removed from IN prior to in vitro integration assays (see below).

(i) Purification under native conditions. A 2-ml chelating Sepharose Fast Flow (Pharmacia Biotech, Piscataway, N.J.) column was precharged with 50 mM $NiSO_4 \cdot 6H_2O$ as previously described (10) and then equilibrated with buffer A. Fraction I was loaded, and the column was washed with approximately 50 ml of buffer A, then with approximately 50 ml of buffer A containing 2 M NaCl–20 mM imidazole, and then with about 50 ml of buffer A containing 60 mM imidazole. The protein was eluted with a linear gradient of 60 mM to 1 M imidazole in buffer A. IN-containing fractions were pooled, EDTA was added to the final concentration of 5 mM, and the protein was dialyzed against 20 mM HEPES (pH 7.6)–1 M NaCl–2 mM EDTA–2 mM β-ME–0.3 M imidazole–10% (wt/vol) glycerol. The His tag was removed from IN by treatment with human thrombin (Sigma, St. Louis, Mo.) essentially as previously described (10). Four vector-derived residues, Gly-Ser-His-Met, remain at the N terminus after cleavage. Thrombin was removed by adsorption to Benzamidine Sepharose 6B (Pharmacia). Cleaved protein was dialyzed against 20 mM HEPES (pH 7.6)–1 mM EDTA–1 M NaCl–10% glycerol–1 mM dithiothreitol and centrifuged at 19,000 × *g* for 10 min. The concentration of IN in the supernatant was adjusted to 0.1 mg/ml in the presence of 10 mM [(3-cholamidopropyl)-dimethylammonio]-1-propanesulfonate (CHAPS), and the protein was dialyzed against buffer C (20 mM HEPES [pH 7.6], 1 mM EDTA, 0.2 M NaCl, 10% glycerol, 1 mM dithiothreitol, 15 mM CHAPS). The dialysate was centrifuged at 19,000 × *g* for 10 min, and the supernatant was concentrated by ultrafiltration in a Centriprep 10 concentrator (Amicon, Inc., Beverly, Mass.) under conditions specified by the manufacturer. Concentrated protein was dialyzed against buffer C and centrifuged at 19,000 × *g* for 10 min, and the soluble IN was frozen in liquid N_2 and stored at −80°C.

WT IN (IN^{WT}) was purified and dialyzed against buffer C as previously described (10, 14, 39).

(ii) Purification under denaturing conditions. Fraction II was loaded over a precharged 2-ml Ni^{2+} chelating column equilibrated with buffer B. The column was washed with approximately 50 ml of buffer B and then with about 50 ml of buffer B containing 20 mM imidazole. Protein was eluted with a linear gradient of 20 to 600 mM imidazole in buffer B. IN-containing fractions were pooled, EDTA was added to the final concentration of 5 mM, and the protein was dialyzed against 6 M Gnd-HCl–20 mM HEPES (pH 7.6)–2 mM EDTA–2 mM β-ME. The concentration of IN was adjusted to 1 mg/ml in dialysis buffer, and an equal volume of buffer containing 1 M NaCl–20 mM HEPES (pH 7.6)–2 mM EDTA–2 mM β-ME was added. The protein was sequentially dialyzed against three buffers which were progressively less denaturing, essentially as previously described (6, 10). The final dialysis was against buffer C. The dialysate was centrifuged at 19,000 × *g* for 10 min, and the supernatant containing soluble refolded IN was treated with thrombin. The flowthrough from the Benzamidine Sepharose column was dialyzed against buffer C and clarified by centrifugation (19,000 × *g* for 10 min), and the IN was frozen in liquid N_2 and stored at −80°C.

Protein crystallography. Crystallization and structure determination of IN residues 50 to 212 of the NL4-3 strain of HIV-1 containing substitutions of Ser for Cys-56 and Lys for Phe-185 will be described elsewhere (12).

IN assays. Three different substrates were used to monitor in vitro biochemical activities. The substrate for assaying 3′ processing activity corresponded to the terminal 21 bp of the U5 end of HIV-1. This DNA was labeled at the 3′ end of the strand which is cleaved by IN. Processing yields different labeled forms of the cleaved GT dinucleotide (10). The substrate for assaying DNA strand transfer activity corresponded to the terminal 30 bp of U5. In this case, the GT dinucleotide normally removed by IN in the 3′ processing reaction is absent, and so strand transfer activity is assayed independent of 3′ processing activity. The third substrate was the Y-mer oligonucleotide, used to measure disintegration activity (9). All three substrates were prepared essentially as previously described (10).

In vitro assay mixtures (16 μl) contained 25 mM morpholinepropanesulfonic acid (pH 7.2), 0.1 mg of bovine serum albumin per ml, 10 mM β-ME, 10% glycerol, 25 nM DNA, 1.7 mM CHAPS, 24 mM NaCl, 7.5 mM $MnCl_2$, and 0.3 μM IN. The concentration of NaCl was varied in some reactions as indicated in the text. Reactions were terminated after 60 min at 37°C and analyzed by electrophoresis on denaturing polyacrylamide sequencing gels as previously described (10). Results were visualized by autoradiography and quantitated by densitometry (IS-1000 Digital Imaging System; Alpha Innotech Corp., San Leandro, Calif.).

Cells and viruses. HeLa cells were grown in Dulbecco modified Eagle medium supplemented to contain 10% fetal calf serum (FCS), 100 U of penicillin G sodium, and 0.1 mg of streptomycin sulfate per ml. Cells (0.7×10^6) were seeded in 10-cm-diameter tissue culture plates 24 h prior to transfection. Virus stocks were prepared by transfecting cells with 35 μg of plasmid in the presence of calcium phosphate (36). Culture supernatants were tested for Mg^{2+}-dependent ^{32}P-RT activity 48 h posttransfection as previously described (16). Supernatants were filtered through 0.45-μm-pore-size nitrocellulose, and equal ^{32}P-RT counts per minute of WT and mutant HIV-1 were used in subsequent infections.

The CEM-12D7 (34) and Jurkat (48) $CD4^+$ T-cell lines were grown in RPMI 1640 supplemented to contain 10% FCS, 100 U of penicillin G sodium, and 0.1 mg of streptomycin sulfate per ml (RPMI-10). Cells (5.0×10^6) were infected with 5.0×10^5 ^{32}P-RT cpm in 0.5 ml of RPMI-10 for 1 h at 37°C prior to addition of 5 ml of RPMI-10. In some cases, 2.5×10^6 cells were infected with 2.5×10^5 ^{32}P-RT cpm in 0.5 ml of RPMI-10. Cultures were fed at 2-day intervals, and aliquots of the medium were assayed for ^{32}P-RT activity. Each virus was tested in at least two independent experiments.

The CD4-LTR/β-gal indicator cell line (26) was maintained in Dulbecco modified Eagle medium supplemented to contain 10% FCS, 100 U of penicillin G sodium, 0.1 mg of streptomycin sulfate, 0.2 mg of G418 sulfate, and 0.1 mg of hygromycin B per ml. Cells were infected, fixed, and stained as previously described (16).

Analysis of HIV-1 proteins. Both cell- and particle-associated HIV-1 proteins were analyzed by radiolabeling transfected HeLa cells and immunoprecipitation with AIDS patient antisera essentially as previously described (16, 18). Results were visualized by fluorography and quantitated by densitometry as described above.

Analysis of viral DNA synthesis. Viral DNA synthesis was analyzed by PCR using primers which amplify sequences from the two-long-terminal-repeat (LTR)-containing circle formed in the nuclei of infected cells. CEM-12D7 cells (5.0×10^6) were infected as described above, and cells were lysed 18 h postinfection as previously described (16). PCR and electrophoresis conditions were as previously described (16).

RESULTS

Mutagenesis strategy. HIV-1 IN is a member of a superfamily of structurally related polynucleotidyltransferase proteins (reviewed in reference 32). These proteins, which include retroviral INs, bacteriophage MuA transposase, RNase H, and RuvC, cut phosphodiester bonds in polynucleotides, generating 3′-OH and 5′-PO_4 ends. The INs and transposases also contain DNA strand transfer activity, which joins the 3′-OH of an integrating donor DNA to a 5′-PO_4 at the site of insertion in a target DNA. The structurally related active-site regions consist of a central five-stranded β sheet flanked by α helices. Conserved carboxylate amino acid residues play critical roles in catalysis. The HIV-1 active-site residues are Asp-64, Asp-116, and Glu-152.

We previously reported the three-dimensional structure of trigonal crystals of the catalytic domain (residues 50 to 212 of the 288-residue protein) of HIV-1 IN to 2.5-Å resolution (13). This structure revealed the locations of two of the three active-site residues, Asp-64 and Asp-116. We recently solved the structure of orthorhombic crystals to 2.0-Å resolution, which revealed the location of Glu-152 (12). Both structures were analyzed to identify amino acid side chains which interact with the side chains of either Asp-64, Asp-116, or Glu-152 (Fig. 1).

(i) Gln-62 and Glu-92. The amide nitrogen of Gln-62 is in hydrogen-bonding distance to a carboxylate oxygen of Asp-64 (Fig. 1A). Glu-92 interacts with the other carboxylate oxygen of Asp-64 through three water molecules (Fig. 1A). Each of these residues is well conserved in an amino acid sequence alignment of retroviral INs: Gln-62 is conserved in 16 of 21 sequences, and Glu-92 is conserved in 18 of the sequences (15). Conservative and nonconservative single amino acid substitutions were introduced at these positions in recombinant IN protein and infectious HIV-1. The roles of these residues in

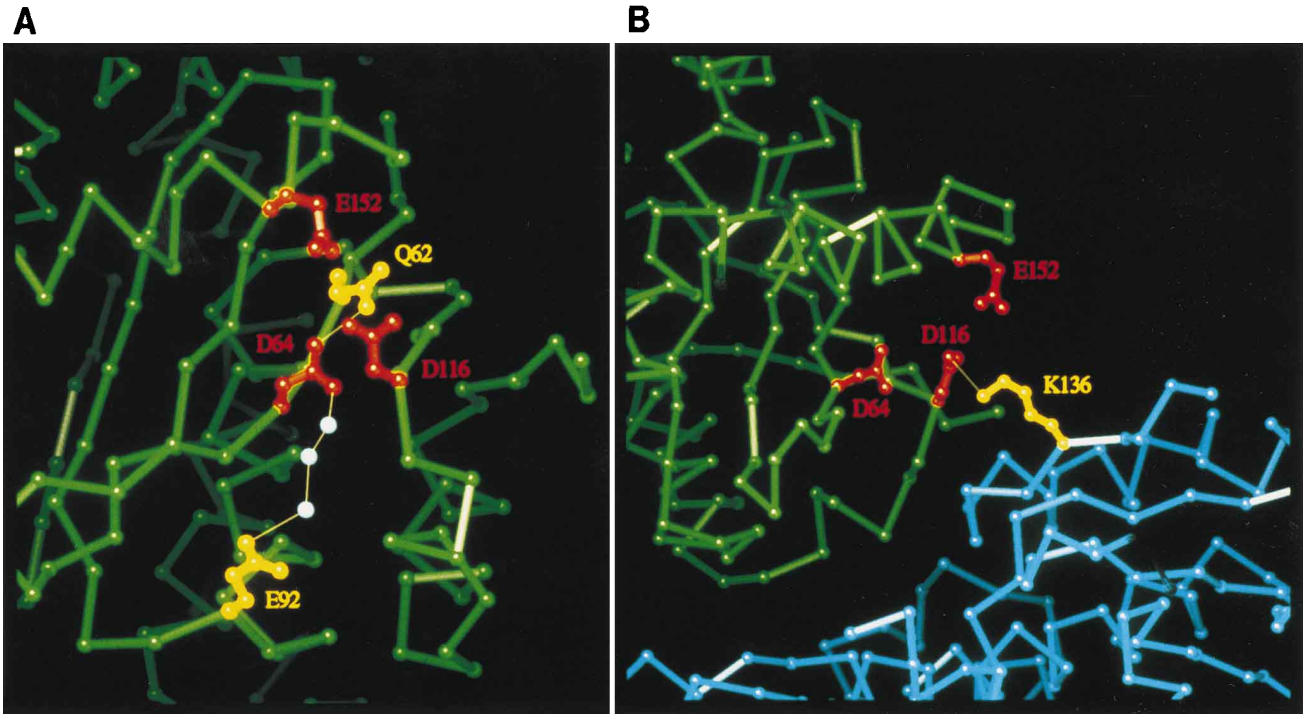

FIG. 1. Structure of the HIV-1 IN active site. (A) Intramolecular side chain interactions. The polypeptide backbone is in green, the side chains of active-site residues Asp-64, Asp-116, and Glu-152 are in red, and the side chains of Gln-62 and Glu-92 are in yellow. Water molecules are in blue, and H bonds are indicated by thin lines. (B) Intermolecular salt bridge. A carboxylate oxygen from one monomer (green backbone) forms an ionic bond (thin line) with the ε-amino group of Lys-136 (yellow) of the second monomer (blue backbone). Other labels are as in panel A. The structure of the orthorhombic crystal is shown (12); each of the interactions is maintained in the trigonal crystal structure (13). The images were drawn by using the program O (24).

integration were assessed after analysis of purified mutant proteins for in vitro biochemical activities and mutant HIV-1 for infectivities in human cell lines.

(ii) Lys-136. There are two dimers in the HIV-1 IN structure, one with an extensive interface and the other with a much smaller contact area (13). Lys-136 interacts with Asp-116 across the minor dimer interface (Fig. 1B), and HIV-1 carrying the substitution of Ala for Lys-136 was previously reported replication defective due to a block in integration (49). Although not well conserved among retroviral INs, Lys-136 is the only non-active-site residue conserved in a structure-based sequence alignment of HIV-1 IN, bacteriophage MuA transposase, and RNase H (33). To further probe the role of Lys-136 in HIV-1 integration, Arg, Glu, and Ala were substituted for Lys in recombinant IN, and Glu was tested in HIV-1. We also analyzed the in vitro activities of recombinant IN containing Ala substitutions for both Lys-136 and Glu-138 ($IN^{K136A/E138A}$), as HIV-1 containing these changes is temperature sensitive for replication (50).

(iii) Phe-185. The substitution of Lys for Phe-185 was required to crystallize the HIV-1 catalytic domain, in part because of a dramatic increase in recombinant IN solubility (13, 23). The ε-amino group of the substituting Lys forms an intermolecular H bond with the main-chain carbonyl of Ala-105 across the larger dimer interface (23). HIV-1 carrying the F185K change ($HIV\text{-}1_{F185K}$), however, is replication defective due to defective virion morphogenesis (22). Is the increased solubility of the IN^{F185K} protein, and/or the two additional H bonds, responsible for the virus assembly defect? His, Leu, and Ala were each substituted for Phe-185 to address these questions. Table 1 lists each of the mutations analyzed in this study.

In vitro biochemical activities. Site-directed mutations were introduced into bacterial expression constructs, and recombinant IN expression was induced in *E. coli*. Each of the mutant proteins was induced to a similar level as IN^{WT}. Cells were lysed in buffer containing 1 M NaCl, and the pellet following centrifugation was extracted with buffer containing 6 M Gnd-HCl. IN-containing fractions were identified by SDS-PAGE, and the mutant proteins were purified under either native or

TABLE 1. In vitro activities of HIV-1 IN mutants[a]

Protein	In vitro activity		
	3′ processing	DNA strand transfer	Disintegration
Q62E	++	++	+++
Q62A	+	+	+++
E92A	+++	+++	+++
E92Q	+++	+++	+++
E92K	+	+	+++
K136R	+++	+++	+++
K136E	+++	+++	+++
K136A	+/−	+/−	+++
K136A/E138A	+++	+++	+++
F185K	+++	+++	ND[b]
F185H	+++	+++	ND
F185L	+++	+++	ND
F185A	+++	+++	ND

[a] +++, 50 to 100% of WT IN activity; ++, 20 to 50% of WT activity; +, 5 to 20% of WT activity; +/−, 1 to 5% of WT activity. Values are averages of at least two independent experiments.

[b] ND, not determined.

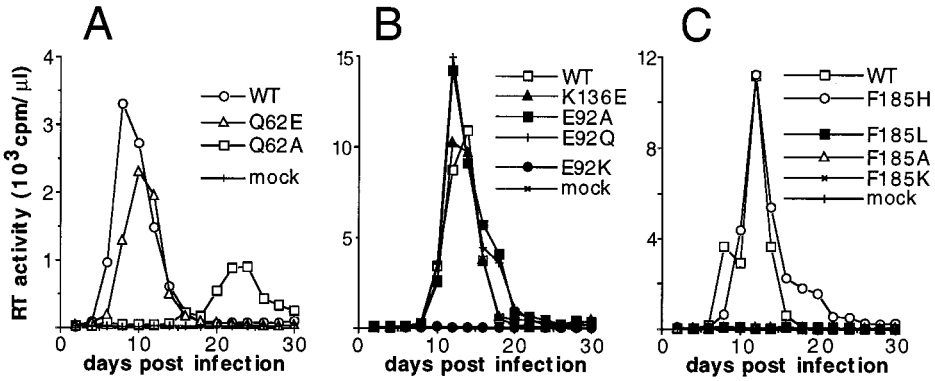

FIG. 2. Replication kinetics of WT and mutant HIV-1. (A) Jurkat cells (2.5×10^6) were infected with 2.5×10^5 ^{32}P-RT cpm of each indicated virus stock, and culture supernatants were monitored for RT activity at the indicated time points. (B and C) Jurkat cells (5.0×10^6) were infected with 5.0×10^5 ^{32}P-RT cpm of the indicated viruses, and culture supernatants were monitored as indicated in panel A. In independent infections, CEM-12D7 cells did not support the replication of HIV-1_{F185L}, HIV-1_{F185A}, or HIV-1_{E92K}. CEM-12D7 cells (5.0×10^6) infected with 5.0×10^5 ^{32}P-RT cpm of HIV-1_{NL4-3}, HIV-1_{Q62E}, or HIV-1_{Q62A} revealed similar growth kinetics, although total virus yields were about twofold lower than those shown in panel A.

denaturing conditions, using one-step nickel affinity chromatography (10, 43). No differences in in vitro integration activities have been seen for WT or mutant IN proteins purified by using the alternative approaches (6, 10, 20, 21).

Two of the 13 recombinant mutant proteins analyzed in this study, IN^{E92K} and $IN^{K136A/E138A}$, were dramatically less soluble than IN^{WT} following lysis in 1 M NaCl buffer. Each of these proteins was purified under denaturing conditions and refolded in the presence of detergent. IN^{F185A} was slightly less soluble than IN^{WT} following lysis, as judged by an approximately fourfold reduction in the amount of protein recovered from the 1 M NaCl lysate following chromatography. IN^{F185A} was also purified in denatured form and refolded. In contrast, IN^{F185H} was more soluble than IN^{WT} following cell lysis, similar to the increase previously reported for IN^{F185K} (22).

In vitro Mn^{2+}-dependent 3′ processing and DNA strand transfer activities were assayed by using oligonucleotide substrates which mimic the U5 end of HIV-1. Many of the purified proteins retained WT levels of in vitro IN activities (Table 1). Notable exceptions were IN^{Q62E}, IN^{Q62A}, IN^{E92K}, and IN^{K136A}. Each of these proteins, however, displayed WT disintegration activity (Table 1).

HIV-1 infectivities. Site-directed mutations were introduced into the pNL4-3 infectious molecular clone of HIV-1 (1). HeLa cells were transfected with plasmid DNA to generate virus stocks. Transfection bypasses early steps in replication, such as reverse transcription, 3′ processing, nuclear localization of the preintegration complex, and DNA strand transfer, any of which may be affected by IN mutations. Each of the mutant plasmids yielded levels of Mg^{2+}-dependent RT activity in HeLa cell supernatants similar to those of the WT plasmid, with the exception of pNL43/F185K. In repeated experiments, this plasmid yielded 15 to 20% of the level of WT activity. After normalization for ^{32}P-RT activity, the infectivity of each virus stock was assessed in Jurkat and CEM-12D7 T-cells by monitoring RT production over a 1-month period.

Cells infected with WT HIV-1_{NL4-3} displayed levels of peak RT activity 8 to 12 days after infection (Fig. 2). Cells infected with HIV-1_{K136E}, HIV-1_{E92Q}, HIV-1_{E92A} (Fig. 2B), and HIV-1_{F185H} (Fig. 2C) supported WT replication kinetics. In repeated experiments, cells infected with HIV-1_{Q62E} displayed peak activities delayed 2 to 4 days from WT-infected cells (Fig. 2A). Cells infected with HIV-1_{Q62A} yielded a much greater delay in peak RT activities, ranging 18 to 24 days from WT-infected cells (Fig. 2A). As previously reported (22), cells infected with HIV-1_{F185K} did not support detectable levels of virus replication (Fig. 2C). Cells infected with HIV-1_{E92K} (Fig. 2B), HIV-1_{F185L}, and HIV-1_{F185A} (Fig. 2C) also showed no signs of virus replication over the course of the experiment.

The infectivity of HIV-1_{NL4-3} and each replication-impaired virus was also measured in a single round by using the multinuclear activation of galactosidase indicator (MAGI) assay (26). CD4-LTR/β-gal indicator cells contain a chromosomal copy of the *lacZ* gene under the control of the HIV-1 promoter. After infection, newly synthesized Tat protein transactivates the promoter and induces β-galactosidase expression. Cells are fixed and stained 48 h postinfection. The infectious titer is the number of cells with blue-stained nuclei per 10^6 ^{32}P-RT cpm of input virus.

Infection of CD4-LTR/β-gal cells with HIV-1_{NL4-3} yielded a titer of approximately 1.8×10^4 (Table 2). The titers of HIV-1_{Q62E} and HIV-1_{Q62A} were 7- to 10-fold lower than that of HIV-1_{NL4-3} (Table 2). Although HIV-1_{E92K} was unable to replicate in infected T-cells, its titer was similar to that of HIV-1_{Q62E}. The titers of HIV-1_{F185L} and HIV-1_{F185A} were approximately 80- and 400-fold, respectively, lower than that of WT (Table 2).

Virion protein composition. In addition to affecting the integration step of the HIV-1 life cycle (2, 8, 16, 28, 29, 31, 35, 40, 42, 49), IN mutations can affect particle assembly and release (2, 5, 16, 22, 40) and reverse transcription (see below). Four of the mutant IN viruses novel to this study either showed grossly delayed replication kinetics (Fig. 2A) or failed to replicate

TABLE 2. MAGI assay with wild-type and mutant HIV-1

Virus	Titer[a] (blue cells/10^6 ^{32}P-RT cpm)
WT NL4-3	18,400
Q62E	2,740
Q62A	1,760
E92K	2,510
F185L	220
F185A	45

[a] Cells which contained dark blue nuclei were counted. Each value is the average from at least three independent infections.

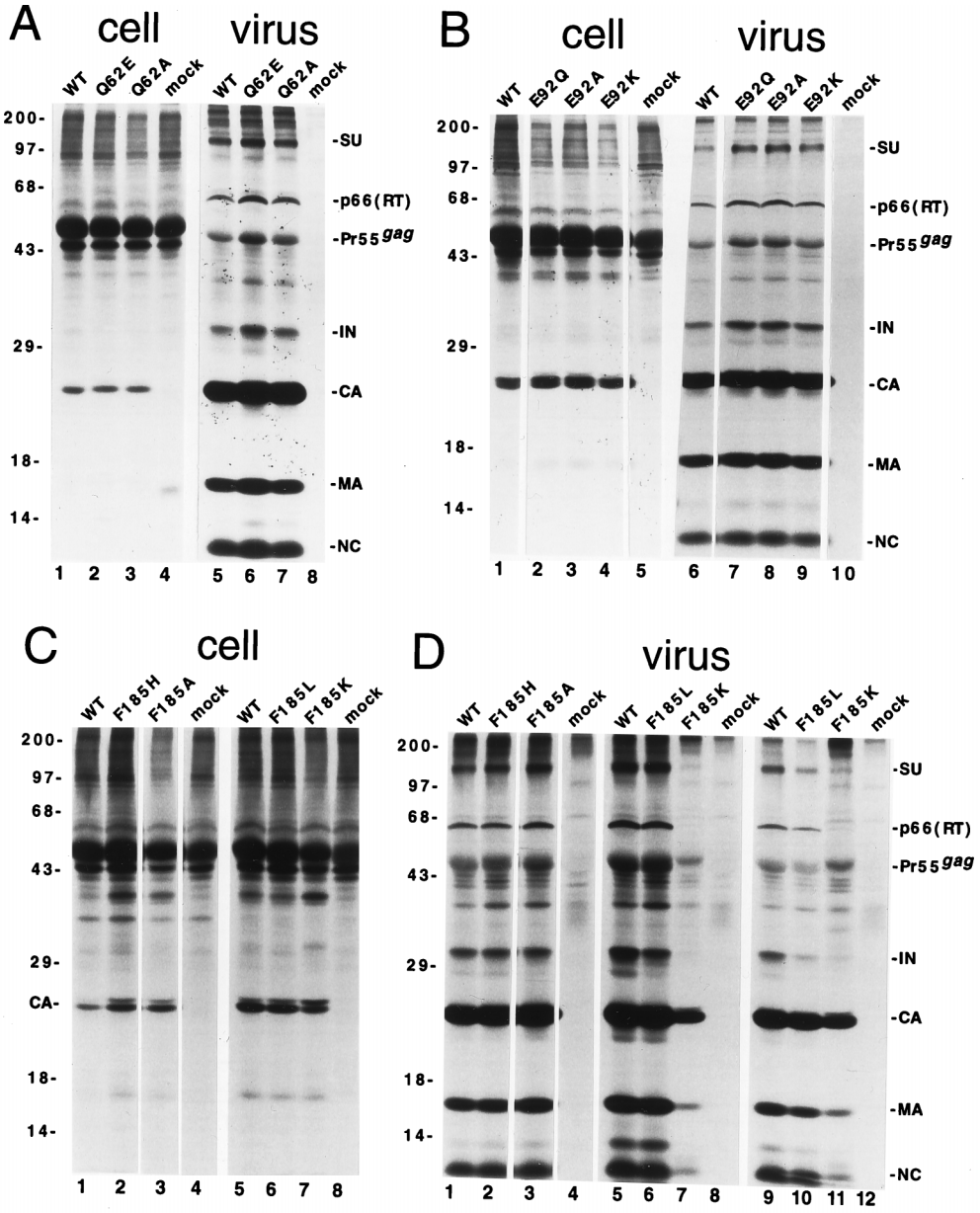

FIG. 3. Analysis of HIV-1 proteins. (A) Cells expressing WT HIV-1_{NL4-3} (lanes 1 and 5), HIV-1_{Q62E} (lanes 2 and 6), and HIV-1_{Q62A} (lanes 3 and 7) were analyzed for cell (lanes 1 to 4)- and particle (lanes 5 to 8)-associated proteins. Lanes 4 and 8 are from mock-transfected cells. The migration positions of HIV-1 proteins are indicated on the right. The migration positions of molecular mass standards are indicated in kilodaltons on the left. (B) Cells expressing WT HIV-1_{NL4-3} (lanes 1 and 6), HIV-1_{E92Q} (lanes 2 and 7), HIV-1_{E92A} (lanes 3 and 8), and HIV-1_{E92K} (lanes 4 and 9) were analyzed for cell (lanes 1 to 5)- and particle- (lanes 6 to 10)-associated proteins. Lanes 5 and 10 were from mock-transfected cells. Other labeling is the same as in panel A. (C) Cell-associated proteins following transfection with either the WT (lanes 1 and 5) or indicated mutant plasmids. Lanes 4 and 8 were from mock-transfected cells. Other labeling is the same as in panel A. (D) Particle-associated proteins from cells expressing WT HIV-1_{NL4-3} (lanes 1, 5, and 10), HIV-1_{F185H} (lane 2), HIV-1_{F185A} (lane 3), HIV-1_{F185L} (lanes 6 and 10), and HIV-1_{F185K} (lanes 7 and 11). Lanes 4, 8, and 12 were from pelleted supernatants of mock-transfected cells. The amount of viral lysate analyzed by immunoprecipitation in lanes 9 to 11 was adjusted for equal ^{32}P-RT cpm. Other labels are the same as in panel A.

in human T-cell lines (Fig. 2B and C). To determine whether virion protein composition or release was affected by these mutations, transfected HeLa cells were radiolabeled, and HIV-1 proteins were visualized in cell lysates and pelleted virions following immunoprecipitation with AIDS patient antisera.

Transfected cells expressing HIV-1_{WT}, HIV-1_{Q62E}, and HIV-1_{Q62A} contained similar amounts of the capsid (CA) protein (Fig. 3A, lanes 1 to 4). Numerous proteins, including the surface (SU) envelope glycoprotein, the p66 subunit of RT, the Pr55^{gag} precursor, IN, CA, matrix (MA), and nucleocapsid (NC), were detected in pelleted HIV-1_{NL4-3} (Fig. 3A, lane 5). HIV-1_{Q62E} and HIV-1_{Q62A} contained each of these proteins at levels similar to the WT level (Fig. 3A, lanes 6 and 7). HIV-1_{E92Q}, HIV-1_{E92A}, and HIV-1_{E92K} also displayed the WT pattern of virion proteins (Fig. 3B, lanes 6 to 10). These results indicate that neither the delayed growth of HIV-1_{Q62A} (Fig. 2A) nor the replication-defective phenotype of HIV-1_{E92K} (Fig. 2B) is due to improper virion assembly or release.

HeLa cells expressing HIV-1_{F185K}, HIV-1_{F185L}, and HIV-

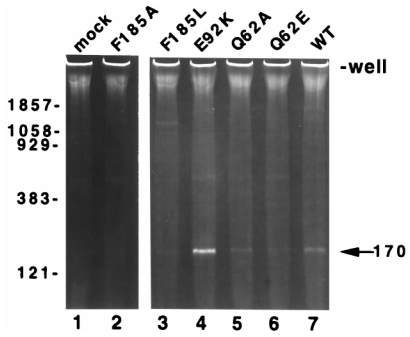

FIG. 4. PCR analysis of the two-LTR-containing circle in CEM-12D7 cells. Reactions in lanes 2 to 6 contained lysates of cells infected with the indicated viruses. Lane 1 contained a lysate from mock-infected cells. The migration positions of DNA standards are indicated in base pairs on the left. The positions of the polyacrylamide gel well and the 170-bp U5/U3 circle junction PCR product are indicated on the right.

1_{F185A} contained roughly similar amounts of the CA protein as cells expressing HIV-1_{NL4-3} and HIV-1_{F185H} (Fig. 3C). As previously reported (22), the Lys substitution affected particle assembly and release. Approximately 10-fold less HIV-1_{F185K} than WT was released (Fig. 3C and D; compare lanes 5 and 7). Normalizing transfected cell supernatants for equal ^{32}P-RT activity prior to immunoprecipitation demonstrated an approximate fivefold reduction in IN relative to CA in HIV-1_{F185K} (Fig. 3C, lane 11). In contrast, HIV-1_{F185A} and HIV-1_{F185L} were efficiently released from transfected cells (Fig. 3D, lanes 3 and 6). HIV-1_{F185A} contained the WT level of virion proteins, while HIV-1_{F185L} contained about twofold less IN compared to CA (Fig. 3D, lanes 6 and 10). Unlike HIV-1_{F185K}, the primary mechanism for the defective phenotypes of HIV-1_{F185L} and HIV-1_{F185A} is apparently not at the particle assembly step of replication.

IN mutations and viral DNA synthesis. Certain HIV-1 IN mutations affect reverse transcription (16, 29, 31, 40, 42). To assess whether any of the mutations in this study affect DNA synthesis, CEM-12D7 cell lysates were analyzed by PCR 18 h after infection, using primers which amplify sequences unique to the two-LTR-containing circular DNA formed in the nuclei of infected cells. This analysis revealed amplified fragments of the appropriate size in cells infected with HIV-1_{NL4-3}, HIV-1_{Q62E}, HIV-1_{Q62A}, HIV-1_{E92K}, and HIV-1_{F185L} but not in cells infected with HIV-1_{F185A} (Fig. 4). The signals from cells infected with HIV-1_{Q62E}, HIV-1_{Q62A}, and HIV-1_{F185L} were consistently less intense than the signal from WT-infected cells. In contrast, cells infected with HIV-1_{E92K} yielded a signal more intense than the signal from WT-infected cells (Fig. 4; compare lanes 4 and 7).

DISCUSSION

Structure-based mutagenesis. Retroviral INs are polynucleotidyltransferases. All members of this structurally related protein superfamily require highly conserved Asp and Glu residues and divalent metal ion for catalysis. In this study, we analyzed two different crystal structures of the HIV-1 IN catalytic domain for interactions at the active site. We hypothesized that such interactions may be important for IN function. Three residues, Gln-62, Glu-92, and Lys-136, were identified as interacting with either active-site residue Asp-64 or active-site residue Asp-116. The roles of these interactions in integration were addressed by analyzing purified mutant proteins for in vitro biochemical activities and mutant HIV-1 for infectivities in human cell lines. The results indicate that none of these interactions is essential for catalysis. It is possible that the participating residues are not in their active configurations in the structures. This is not surprising given that neither divalent metal ion or DNA substrate is present in the crystals. It is tempting to speculate that some of these interactions play a more significant role in crystal packing than in IN function. It has also been suggested that the structure of the MuA transposase catalytic domain, which was solved in the absence of DNA and metal, represents an inactive conformation (33).

Integration-minus HIV-1. Our structure-based mutagenesis strategy uncovered novel HIV-1 IN mutant phenotypes. The substitution of Lys for Glu-92 reduced in vitro 3′ processing and DNA strand transfer activities 5- to 10-fold and blocked HIV-1 growth in both Jurkat and CEM-12D7 T-cells. HIV-1_{E92K} behaved like previously described IN active-site mutants (2, 16, 49): virus assembly and reverse transcription were unaffected by the mutation, infected T cells contained more circular DNA than WT-infected cells, and a relatively high titer was observed in the MAGI assay. This phenotype is expected for a virus which is blocked specifically at the integration step of the life cycle. As suggested for active-site mutants, it is possible that infected CD4-LTR/β-gal cells express Tat from unintegrated viral DNA. Because of the similar viral phenotype, we propose that IN^{E92K} is also catalytically inactive in infected cells. What function may be altered in cells infected with HIV-1_{E92K}? Since recombinant IN^{E92K} protein displayed partial in vitro 3′ processing and DNA strand transfer activities, as well as the WT level of disintegration activity, we speculate that DNA recognition by the mutant IN may be impaired in infected cells. Experiments to test this hypothesis are under way.

Minor dimer interface. Results of in vitro complementation experiments have shown that the catalytic domain plays an important role in the functional multimerization of HIV-1 IN (14, 45). There are two dimers in the HIV-1 structures; one has a large solvent-excluded interface of approximately 1,300 Å, while the other interface is much smaller (13). It seems likely that the larger interface is biologically relevant, as avian sarcoma virus forms a similar dimer (4). The active sites in this dimer are separated by about 35 Å in HIV-1, which is about twice the distance required to integrate two viral ends 5 bp (approximately 17 Å) apart (13). Lys-136 and Asp-116 interact across the smaller dimer interface, and HIV-1 carrying the substitution of Ala for Lys-136 is replication defective due to a block in integration (49). We found that mutants carrying Glu for Lys-136 displayed WT levels of in vitro and in vivo activities, suggesting that the Lys-136–Asp-116 interaction, and by extension the dimer interface which it helps form, is not biologically relevant. It is possible that Lys-136 and Asp-116 are in their native configurations in the structures, and the minor dimer interface is solely the result of crystal packing.

It is unclear why HIV-1_{K136E} replicated with WT kinetics, since HIV-1_{K136A} is replication defective (49). IN^{K136A} may not form functional protein-protein and/or IN-DNA interactions in the viral preintegration complex. Alternatively, the different replication profiles may simply reflect in vitro integration activities, as IN^{K136A} displayed only 1 to 5% of the level of IN^{WT} and IN^{K136E} 3′ processing and DNA strand transfer (Table 1). Substituting Ala for Glu-138 in IN^{K136A} restored these activities to nearly WT levels (Table 1). The 3′ processing, DNA strand transfer, and disintegration activities of IN^{WT}, IN^{K136A}, and $IN^{K136A/E138A}$ were tested at 30 and 42°C. As previously reported (46), IN^{WT} displayed greater 3′ processing and DNA strand transfer activities at the elevated temperature. IN^{K136A} and $IN^{K136A/E138A}$ each supported more

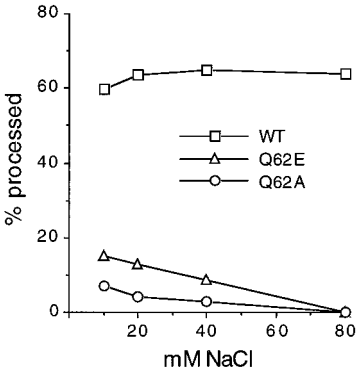

FIG. 5. NaCl affects the 3′ processing activity of IN^{Q62E} more than that of IN^{WT}. 3′ processing reactions contained the indicated IN protein and NaCl concentration. In repeated experiments, the activities of IN^{Q62E} and IN^{Q62A} were undetectable (<0.1% of substrate converted to products) in reactions containing 80 mM NaCl. IN^{E92K} displayed 5 to 20% of IN^{WT} 3′ processing activity at each indicated NaCl concentration. The 3′ processing activities of both IN^{WT} and IN^{E92K} were undetectable in reactions containing 160 mM NaCl.

3′ processing activity at 42°C than at 30°C but about twofold less strand transfer activity at 42°C than at 30°C (17). We conclude that the in vitro DNA strand transfer activity of $IN^{K136A/E138A}$ is marginally temperature sensitive. These results are consistent with the previous report that HIV-$1_{K136A/E138A}$ is blocked at the nonpermissive temperature in infected cells at a step in the life cycle other than integration (50).

IN solubility and HIV-1 replication. The substitution of Lys for Phe-185 dramatically increased the solubility of recombinant HIV-1 IN and was required to crystallize the catalytic domain (13, 23). HIV-1 carrying this change, however, was replication defective due to defective virus assembly (22). Substituting His for Phe-185 increased the solubility of full-length IN protein similarly to the increase reported for IN^{F185K}, and HIV-1_{F185H} replicated with WT kinetics. This shows that increased IN solubility is not necessarily detrimental to particle assembly or replication. However, the extra H bonds in the HIV-1 structure between the substituting lysines and the main-chain carbonyls of Ala-105 might contribute to the HIV-1_{F185K} particle assembly defect. Bujacz et al. (3) recently solved the crystal structure of the HIV-1 catalytic domain containing His in place of Phe-185. The larger dimer interface is intact in that structure, and intermolecular H bonds form between each His-185 and Ala-105. We infer that neither the increased solubility of IN^{F185K} nor the extra H bonds in the dimer necessarily contribute to the particle assembly defect of HIV-1_{F185K}. HIV-1_{F185L} and HIV-1_{F185A} were replication defective and displayed nearly normal virion protein composition but reduced DNA synthesis and MAGI assay titers. Based on these results, we suggest that an amino acid side chain with aromatic behavior at position 185 may be important for proper reverse transcription and HIV-1 replication. Mutants of Phe-185 display quite different replication phenotypes considering that each recombinant IN protein displays nearly WT levels of in vitro integration activities.

IN activity and HIV-1 replication. Mutants carrying either Glu or Ala for Gln-62 displayed partial activities in vitro and in vivo. Interestingly, HIV-1_{Q62E} replicated similarly to HIV-1_{NL4-3}, despite approximately fivefold reductions in in vitro 3′ processing and DNA strand transfer activities (Table 1). There are numerous examples of mutations which affect virus growth more than recombinant IN function, which in many cases is explained by the pleiotropic effects of IN mutations on virus assembly and reverse transcription (8, 16, 22, 29, 31, 40, 42). However, reports of the opposite effect (i.e., mutations which affect in vitro IN activities more than virus growth) are rare. One mutation which in part displays this phenotype is the substitution of Gly for Asn-120. In this case, in vitro 3′ processing and DNA strand transfer activities are reduced 2- to 10-fold, and the titer of pseudotyped HIV-1 is reduced about 30-fold (29). Altering the concentration of NaCl in in vitro 3′ processing reactions highlights the defective nature of the IN^{Q62E} enzyme reported here. IN^{Q62E} displayed about 20% of IN^{WT} 3′ processing activity in reactions containing 20 mM NaCl (Fig. 5). Whereas the activity of IN^{WT} in mixtures containing 80 mM NaCl was similar to the activity at 20 mM NaCl, the activity of IN^{Q62E} was undetectable (<0.1% of substrate converted to products) at 80 mM NaCl (Fig. 5). The substitution of Glu for Gln-62 is the most striking example of an IN mutation which affects in vitro activities more than virus replication. Thus, these studies support the conclusion that HIV-1 is competent to replicate in T-cell lines with less than the WT level of IN activity. This result has important implications for drug discovery efforts, as compounds identified by using in vitro assays which inhibit IN function may have little or no effect on HIV-1 replication. Future studies of IN mutants should guide the development of antiviral agents directed against this critical HIV-1 enzyme.

ACKNOWLEDGMENTS

We thank D. Gabuzda, H. Gottlinger, and J. Sodroski for critical reading of the manuscript, E. Freed for CEM-12D7 cells, A. Wlodawer for sharing results prior to publication, and R. Craigie, in whose lab this project was started. The following reagents were obtained through the AIDS Research and Reference Reagent Program, Division of AIDS, NIAID, NIH: CD4-LTR/β-gal cells from Michael Emerman and AIDS patient antisera from Alfred Prince.

This work was supported in part by the NIH Intramural AIDS Targeted Antiviral Program (F.D.), by funds from the G. Harold and Leila Y. Mathers foundation (A.E.), and by NIH grant AI39394 (A.E.). Y.L. is a WHO/PAHO Research Fellow.

REFERENCES

1. **Adachi, A., H. E. Gendelman, S. Koenig, T. Folks, R. Willey, A. Rabson, and M. A. Martin.** 1986. Production of acquired immunodeficiency syndrome-associated retrovirus in human and non-human cells transfected with an infectious molecular clone. J. Virol. **59:**284–291.
2. **Ansari-Lari, M. L., L. A. Donehower, and R. A. Gibbs.** 1995. Analysis of human immunodeficiency virus type 1 integrase mutants. Virology **211:**332–335.
3. **Bujacz, G., J. Alexandratos, Q. Zhou-Liu, C. Clement, and A. Wlodawer.** 1996. The catalytic domain of human immunodeficiency virus integrase: ordered active site in the F185H mutant. FEBS Lett. **398:**175–178.
4. **Bujacz, G., M. Jaskolski, J. Alexandratos, A. Wlodawer, G. Merkel, R. A. Katz, and A. M. Skalka.** 1995. High-resolution structure of the catalytic domain of avian sarcoma virus integrase. J. Mol. Biol. **253:**336–346.
5. **Bukovsky, A., and H. Göttlinger.** 1996. Lack of integrase can markedly affect human immunodeficiency virus type 1 particle production in the presence of an active viral protease. J. Virol. **70:**6820–6825.
6. **Bushman, F. D., A. Engelman, I. Palmer, P. Wingfield, and R. Craigie.** 1993. Domains of the integrase protein of human immunodeficiency virus type 1 responsible for polynucleotidyl transfer and zinc binding. Proc. Natl. Acad. Sci. USA **90:**3428–3432.
7. **Bushman, F. D., T. Fujiwara, and R. Craigie.** 1990. Retroviral DNA integration directed by HIV integration protein in vitro. Science **249:**1555–1558.
8. **Cannon, P. M., W. Wilson, E. Byles, S. M. Kingsman, and A. J. Kingsman.** 1994. Human immunodeficiency virus type 1 integrase: effect on viral replication of mutations at highly conserved residues. J. Virol. **68:**4768–4775.
9. **Chow, S. A., K. A. Vincent, V. Ellison, and P. O. Brown.** 1992. Reversal of integration and DNA splicing mediated by integrase of human immunodeficiency virus. Science **255:**723–726.
10. **Craigie, R., A. B. Hickman, and A. Engelman.** 1995. Integrase, p. 53–71. *In* J. Karn (ed.), HIV, vol. II. A practical approach. Oxford University Press, Oxford, England.
11. **Drelich, M., R. Wilhelm, and J. Mous.** 1992. Identification of amino acid

residues critical for endonuclease and integration activities of HIV-1 IN protein in vitro. Virology **188:**459–468.
12. **Dyda, F., A. B. Hickman, T. M. Jenkins, R. Craigie, and D. R. Davies.** Structure of the catalytic domain of HIV-1 integrase at 2.0 Å resolution. Submitted for publication.
13. **Dyda, F., A. B. Hickman, T. M. Jenkins, A. Engelman, R. Craigie, and D. R. Davies.** 1994. Crystal structure of the catalytic domain of HIV-1 integrase: similarity to other polynucleotidyl transferases. Science **266:**1981–1986.
14. **Engelman, A., F. D. Bushman, and R. Craigie.** 1993. Identification of discrete functional domains of HIV-1 integrase and their organization within an active multimeric complex. EMBO J. **12:**3269–3275.
15. **Engelman, A., and R. Craigie.** 1992. Identification of conserved amino acid residues critical for human immunodeficiency virus type 1 integrase function in vitro. J. Virol. **66:**6361–6369.
16. **Engelman, A., G. Englund, J. M. Orenstein, M. A. Martin, and R. Craigie.** 1995. Multiple effects of mutations in human immunodeficiency virus type 1 integrase on viral replication. J. Virol. **69:**2729–2736.
17. **Engelman, A., and Y. Liu.** Unpublished observations.
18. **Freed, E. O., J. M. Orenstein, A. J. Buckler-White, and M. A. Martin.** 1994. Single amino acid changes in the human immunodeficiency virus type 1 matrix protein block virus particle formation. J. Virol. **68:**5311–5320.
19. **Goodarzi, G., G.-J. Im, K. Brackmann, and D. P. Grandgenett.** 1995. Concerted integration of retrovirus-like DNA by human immunodeficiency virus integrase. J. Virol. **69:**6090–6097.
20. **Goulaouic, H., and S. A. Chow.** 1996. Directed integration of viral DNA mediated by fusion proteins consisting of human immunodeficiency virus type 1 integrase and *Escherichia coli* LexA protein. J. Virol. **70:**37–46.
21. **Grandgenett, D. P., and G. Goodarzi.** 1994. Folding of the multidomain human immunodeficiency virus type 1 integrase. Protein Sci. **3:**888–897.
22. **Jenkins, T. M., A. Engelman, R. Ghirlando, and R. Craigie.** 1996. A soluble active mutant of HIV-1 integrase: involvement of both the core and C-terminal domains in multimerization. J. Biol. Chem. **271:**7712–7718.
23. **Jenkins, T. M., A. B. Hickman, F. Dyda, R. Ghirlando, D. R. Davies, and R. Craigie.** 1995. Catalytic domain of human immunodeficiency virus type 1 integrase: identification of a soluble mutant by systematic replacement of hydrophobic residues. Proc. Natl. Acad. Sci. USA **92:**6057–6061.
24. **Jones, T. A., J. Y. Zou, S. W. Cowan, and M. Kjeldgaard.** 1991. Improved methods for building protein models in electron density maps and the location of errors in these models. Acta Crystallogr. **A47:**110.
25. **Katz, R. A., and A. M. Skalka.** 1994. The retroviral enzymes. Annu. Rev. Biochem. **63:**133–173.
26. **Kimpton, J., and M. Emerman.** 1992. Detection of replication-competent and pseudotyped human immunodeficiency virus with a sensitive cell line on the basis of activation of an integrated β-galactosidase gene. J. Virol. **66:** 2232–2239.
27. **Kulkosky, J., K. S. Jones, R. A. Katz, J. P. G. Mack, and A. M. Skalka.** 1992. Residues critical for retroviral integrative recombination in a region that is highly conserved among retroviral/retrotransposon integrases and bacterial insertion sequence transposases. Mol. Cell. Biol. **12:**2331–2338.
28. **Lafemina, R. L., C. L. Schneider, H. L. Robbins, P. L. Callahan, K. LeGrow, E. Roth, W. A. Schleif, and E. A. Emini.** 1992. Requirement of active human immunodeficiency virus type 1 integrase enzyme for productive infection of human T-lymphoid cells. J. Virol. **66:**7414–7419.
29. **Leavitt, A. D., G. Robles, N. Alesandro, and H. E. Varmus.** 1996. Human immunodeficiency virus type 1 integrase mutants retain in vitro integrase activity yet fail to integrate DNA efficiently during infection. J. Virol. **70:** 721–728.
30. **Leavitt, A. D., L. Shiue, and H. E. Varmus.** 1993. Site-directed mutagenesis of HIV-1 integrase demonstrates differential effects on integrase function in vitro. J. Biol. Chem. **268:**2113–2119.
31. **Masuda, T., V. Planelles, P. Krogstad, and I. S. Y. Chen.** 1995. Genetic analysis of human immunodeficiency virus type 1 integrase and the U3 *att* site: unusual phenotype of mutants in the zinc finger-like domain. J. Virol. **69:**6687–6696.
32. **Rice, P., R. Craigie, and D. R. Davies.** 1996. Retroviral integrases and their cousins. Curr. Opinion Struct. Biol. **6:**76–83.
33. **Rice, P. A., and K. Mizuuchi.** 1995. Structure of the bacteriophage Mu transposase core: a common structural motif for DNA transposition and retroviral integration. Cell **82:**209–220.
34. **Ross, E. K., A. J. Buckler-White, A. Rabson, G. Englund, and M. A. Martin.** 1991. Contribution of NF-κB and Sp1 binding motifs to the replicative capacity of human immunodeficiency virus type 1: distinct patterns of viral growth are determined by T-cell types. J. Virol. **65:**4350–4358.
35. **Sakai, H., M. Kawamura, J.-I. Sakuragi, S. Sakuragi, R. Shibata, A. Ishimoto, N. Ono, S. Ueda, and A. Adachi.** 1993. Integration is essential for efficient gene expression of human immunodeficiency virus type 1. J. Virol. **67:**1169–1174.
36. **Sambrook, J., E. F. Fritsch, and T. Maniatis.** 1989. Molecular cloning: a laboratory manual, 2nd ed. Cold Spring Harbor Laboratory Press, Cold Spring Harbor, N.Y.
37. **Sanger, F., S. Nicklen, and A. R. Coulson.** 1977. DNA sequencing with chain-terminating inhibitors. Proc. Natl. Acad. Sci. USA **74:**5463–5467.
38. **Schauer, M., and A. Billich.** 1992. The N-terminal region of HIV-1 integrase is required for integration activity, but not for DNA binding. Biochem. Biophys. Res. Commun. **185:**874–880.
39. **Sherman, P. A., and J. A. Fyfe.** 1990. Human immunodeficiency virus integration protein expressed in *Escherichia coli* possesses selective DNA cleaving activity. Proc. Natl. Acad. Sci. USA **87:**5119–5123.
40. **Shin, C., B. Taddeo, W. A. Haseltine, and C. M. Farnet.** 1994. Genetic analysis of the human immunodeficiency virus type 1 integrase protein. J. Virol. **68:**1633–1642.
41. **Studier, F. W., and B. A. Moffatt.** 1986. Use of bacteriophage T7 RNA polymerase to direct selective high-level expression of cloned genes. J. Mol. Biol. **189:**113–130.
42. **Taddeo, B., W. A. Haseltine, and C. M. Farnet.** 1994. Integrase mutants of human immunodeficiency virus type 1 with a specific defect in integration. J. Virol. **68:**8401–8405.
43. **van Dyke, M. W., M. Sirito, and M. Sawadogo.** 1992. Single-step purification of bacterially expressed polypeptides containing an oligo-histidine domain. Gene **111:**99–104.
44. **van Gent, D. C., A. A. M. Oude Groeneger, and R. H. A. Plasterk.** 1992. Mutational analysis of the integrase protein of human immunodeficiency virus type 2. Proc. Natl. Acad. Sci. USA **89:**9598–9602.
45. **van Gent, D. C., C. Vink, A. A. M. Oude Groeneger, and R. H. A. Plasterk.** 1993. Complementation between HIV integrase proteins mutated in different domains. EMBO J. **12:**3261–3267.
46. **Vincent, K. A., V. Ellison, S. A. Chow, and P. O. Brown.** 1993. Characterization of human immunodeficiency virus type 1 integrase expressed in *Escherichia coli* and analysis of variants with amino-terminal mutations. J. Virol. **67:**425–437.
47. **Vink, C., A. A. M. Oude Groeneger, and R. H. A. Plasterk.** 1993. Identification of the catalytic and DNA-binding region of human immunodeficiency virus type 1 integrase protein. Nucleic Acids Res. **21:**1419–1425.
48. **Weiss, A., R. L. Wiskocil, and J. D. Stobo.** 1984. The role of T3 surface molecules in the activation of human T cells: a two-stimulus requirement for IL 2 production reflects events occurring at a pretranslational level. J. Immunol. **133:**123–128.
49. **Wiskerchen, M., and M. A. Muesing.** 1995. Human immunodeficiency virus type 1 integrase: effects of mutations on viral ability to integrate, direct gene expression from unintegrated viral DNA templates, and sustain propagation in primary cells. J. Virol. **69:**376–386.
50. **Wiskerchen, M., and M. A. Muesing.** 1995. Identification and characterization of a temperature-sensitive mutant of human immunodeficiency virus type 1 by alanine scanning mutagenesis of the integrase gene. J. Virol. **69:**597–601.